



Fermi National Accelerator Laboratory

FERMILAB-Pub-95/040

Hyperon Radiative Decays

J. Lach

*Fermi National Accelerator Laboratory
P.O. Box 500, Batavia, Illinois 60510*

P. Zenczykowski

*Institute of Nuclear Physics
Radzikowskiego 152, 31-342 Krakow, Poland*

March 1995

Accepted for publication in *International Journal of Modern Physics A*



Operated by Universities Research Association Inc. under Contract No. DE-AC02-76CHO3000 with the United States Department of Energy

Disclaimer

This report was prepared as an account of work sponsored by an agency of the United States Government. Neither the United States Government nor any agency thereof, nor any of their employees, makes any warranty, express or implied, or assumes any legal liability or responsibility for the accuracy, completeness, or usefulness of any information, apparatus, product, or process disclosed, or represents that its use would not infringe privately owned rights. Reference herein to any specific commercial product, process, or service by trade name, trademark, manufacturer, or otherwise, does not necessarily constitute or imply its endorsement, recommendation, or favoring by the United States Government or any agency thereof. The views and opinions of authors expressed herein do not necessarily state or reflect those of the United States Government or any agency thereof.

HYPERON RADIATIVE DECAYS

J. LACH

*Fermilab, PO Box 500 MS 220
Batavia, IL 60510, USA*

P. ŻENCZYKOWSKI

*Institute of Nuclear Physics
Radzikowskiego 152
31-342 Krakow, Poland*

ABSTRACT

We review the experimental and theoretical status of weak radiative hyperon decays. Our discussion centers around a controversy over the validity of Hara's theorem originally expected to be respected by these decays. After presenting the hadron-level theorem we describe experiments that have provided convincing evidence against its applicability to these decays. In the theoretical part we juxtapose the hadron-level and quark-level approaches and discuss the violation of Hara's theorem in the latter. We review quark-model phenomenology which offers a promising description of experimental data. Measurements that should be done to settle the theoretical controversy are pinpointed. The importance of radiative hyperon decays in understanding the nonlocal composite nature of hadrons is stressed.

1. Introduction

Hyperon radiative decays exhibit the full interplay of the electromagnetic, weak, and strong interactions. One would think that because of their simple two body kinematics: just the decay of one baryon into another with the emission of a photon, they should be amenable to insightful theoretical analysis and clean experimental probing. In fact, they have proved to be a challenge to both the theorist and experimenter.

These strangeness changing decays are induced by the weak interactions but their final state photon ensures that the electromagnetic forces are also involved. Since baryons are strongly interacting particles, the strong force is also important.

The baryon octet provides us with multiple reactions of this class with varying quark content of the initial and final state baryons. These are the decays

$$\begin{array}{ll} \Sigma^+ \rightarrow p \gamma & \Xi^0 \rightarrow \Sigma^0 \gamma \\ \Sigma^0 \rightarrow n \gamma & \Xi^0 \rightarrow \Lambda^0 \gamma \\ \Lambda^0 \rightarrow n \gamma & \Xi^- \rightarrow \Sigma^- \gamma \end{array} \quad (1)$$

Because the weak decay, $\Sigma^0 \rightarrow n \gamma$, is completely overwhelmed by the simpler strangeness conserving electromagnetic decay, $\Sigma^0 \rightarrow \Lambda^0 \gamma$, it has not been observed. Except for this decay, all decays of the baryon octet have received major attention and been observed.

Although decays from the baryon decuplet are also of great interest, the only member of the decuplet with a sufficiently long lifetime to make it accessible to experimental study is the Ω^- . Its decay to a member of the octet

$$\Omega^- \rightarrow \Xi^- \gamma$$

is expected to be dominant.

So far, however, only upper limits have been put on its branching fraction (R). The Ω^- decay to a member of the decuplet

$$\Omega^- \rightarrow \Xi^*(1530) \gamma$$

is expected to have a branching fraction an order of magnitude smaller than the octet mode.^{1,2}

The weak radiative hyperon decays (WRHD) pose significant experimental challenges. They have small branching fractions, $\approx 10^{-3}$, and copious photon backgrounds due to their more abundant decay modes involving $\pi^0 \rightarrow \gamma\gamma$. The most sensitive tests require the use of polarized hyperons. Modern hyperon beams have provided effective tools for overcoming these difficulties.

Theoretical difficulties manifest themselves in a long history of unsuccessful attempts to describe data in hadron level approaches and in the appearance of a basic conflict between these approaches and the quark model. For these reasons WRHD have been regarded as "the last low q^2 frontier of weak interaction physics³", "unsolved puzzle⁴", "the long-standing $\Sigma^+ \rightarrow p\gamma$ puzzle⁵", "a puzzle which has so far defied a simple and widely accepted solution²", and "a long standing discrepancy⁶". Clearly, there are still many unsolved questions in the domain of low q^2 weak interaction physics (for example the origin of the $\Delta I=1/2$ rule, etc.). The problem of WRHD seems to be of a more fundamental nature, however.

Yet, significant experimental and theoretical progress has been made in the last ten years. The aim of this paper is to review the present status of both the theory and experiments, discuss what we believe are existing problems and point to promising future directions.

We follow this introduction with Section 2, a brief discussion of the experimental techniques, and present the basic measurements in Table 2.1. This is followed by Section 3 devoted to Hara's theorem in which we try to crystallize the nature of the problem. Before embarking on a discussion of the experimental results, we present theoretical lower bounds on the WRHD branching fractions in Section 4. These bounds are imposed by unitarity and therefore they are very reliable.

In sections 3 and 4 we develop general theoretical arguments and explore the nature of the controversy. In Section 5, we return for a more detailed description of the experimental measurements. Section 6 develops the hadron level formalism for nonleptonic and radiative hyperon decays, Section 7 explores the phenomenology of the

standard approaches, Section 8 looks at the single quark processes, Section 9 considers other approaches and, finally, we present our conclusions in Section 10.

2. Experimental Techniques and Data Summary

Hyperon radiative decay measurements consist of branching fractions and asymmetry parameters. The measurement of branching fractions requires identification of the hyperons and of the unique radiative decay final state. Although limited statistically, reliable measurements came from early bubble chamber experiments. More recent measurements have employed electronic techniques and most have relied on high energy hyperon beams at Fermilab.

Hyperon beams can provide substantial fluxes of hyperons; furthermore, they can be produced with significant polarization. The direction and magnitude of these polarizations can be controlled thus providing an important tool for the evaluation of systematic uncertainties. These high energy hyperon beams with their easily controlled polarizations have also allowed us to make precision measurements of hyperon static properties.

They have allowed us to study polarization effects in Σ^- beta decay,⁷ high statistics weak radiative decays,⁸ and to make precision measurements of hyperon magnetic moments.⁹⁻¹¹ Hyperon polarization has provided an extremely useful tool for the study of hyperon fundamental properties, although the production mechanism which produces these polarizations is not well understood. A number of reviews describing hyperon beams and the physics programs that have utilized them are available.¹²⁻¹⁵

In recent years it has become clear that hyperon polarization itself is a complex process whose energy and P_t dependence is different¹⁶⁻¹⁹ for each of the hyperons. This has provided significant challenges to our theoretical understanding of polarization mechanisms.

Table 2.1 shows the present experimental status of weak radiative hyperon decays. Not included are some early experiments which have presented upper limits that have been superseded by more recent experiments which have observed the decay. The newer measurements are consistent with the previously measured limits.

In Table 2.1, we list the experimental branching fractions (R), asymmetry parameters (α), number of events, year and place of measurement, and refer to the experimental group by the first author. We quote both the statistical and systematic uncertainty (in that order) for each measurement if available. For those decays where more than one measurement exists, we first combine the statistical and systematic uncertainties quadratically and then form the weighted mean for each set of measurements.

The $\Sigma^+ \rightarrow p\gamma$ reaction was the first WRHD to be observed and stimulated the controversy that is still with us. In Table 2.1 we have not included $\Sigma^+ \rightarrow p\gamma$ measurements which contain less than 25 events. These are early emulsion²⁰ and bubble

Table 2.1 Hyperon Radiative Decay Measurements

	$R \times 10^{-3}$	α	Events	Year	Group
$\Sigma^+ \rightarrow p\gamma$	$1.20 \pm 0.06 \pm 0.05$		31901	1994	Fermilab, Timm ³⁶
		$-0.720 \pm 0.086 \pm 0.045$	34754	1992	Fermilab, Foucher ⁸
	$1.45 \pm 0.20^{+0.11}_{-0.22}$		408	1989	BNL, Hessey ³⁷
	1.30 ± 0.15	$-0.86 \pm 0.13 \pm 0.04$	190	1987	KEK, Kobayashi ³⁸
	1.27 ± 0.17		155	1985	CERN, Biagi ³⁹
	1.09 ± 0.20	$-0.53^{+0.38}_{-0.36}$	30 (R) 46 (α)	1980	CERN, Manz ²⁵
	1.42 ± 0.26	$s -1.03^{+0.52}_{-0.42}$	31 (R) 61 (α)	1969	LBL, Gershwin ²⁴
	1.23 ± 0.06	-0.76 ± 0.08	Combined	Weighted	Mean
	1.75 ± 0.15		1816	1993	BNL, Larsen ²⁷
	1.02 ± 0.33		24	1986	CERN, Biagi ²⁹
$\Lambda \rightarrow n\gamma$	1.63 ± 0.14		Combined	Weighted	Mean
$\Xi^0 \rightarrow \Lambda\gamma$	$1.06 \pm 0.12 \pm 0.11$	0.43 ± 0.44	116 (R) 87 (α)	1990	Fermilab, James ³²
	5 ± 5		1	1974	BNL, ³⁴
	1.06 ± 0.16	0.43 ± 0.44	Combined	Weighted	Mean
$\Xi^0 \rightarrow \Sigma^0\gamma$	$3.56 \pm 0.42 \pm 0.10$	$0.20 \pm 0.32 \pm 0.05$	85	1989	Fermilab, Teige ³³
	< 8.0			1988	BNL, Bensinger ⁴⁰
	3.56 ± 0.43	0.20 ± 0.32	Combined	Weighted	Mean
$\Xi^- \rightarrow \Sigma^- \gamma$	$0.122 \pm 0.023 \pm 0.006$	1.0 ± 1.3	211	1994	Fermilab, Dubbs ³⁰
	0.23 ± 0.10		~ 10	1987	CERN Biagi ³¹
	0.128 ± 0.023	1.0 ± 1.3	Combined	Weighted	Mean
$\Omega^- \rightarrow \Xi^- \gamma$	< 0.46			1994	Fermilab, Albuquerque ³⁵
	< 2.2			1984	CERN, Bourquin ⁴¹

chamber²¹⁻²³ measurements. Some of the branching fraction measurements^{24,25} quote their results as the ratio ($\Sigma^+ \rightarrow p\gamma / \Sigma^+ \rightarrow p\pi^0$). We have converted²⁶ these to absolute branching fractions. Considering the difficulty of these experiments, the measurements are in remarkably good agreement.

The decay rate for $\Lambda^0 \rightarrow n\gamma$ has been observed by two groups, one working at Brookhaven National Laboratory (BNL) and the other working at CERN. The results from the BNL group^{27,28} are contained in two papers, the more recent²⁷ includes the data from the earlier.²⁸ Results from the CERN²⁹ and BNL experiments differ by about 2.0 σ .

The decay $\Xi^- \rightarrow \Sigma^- \gamma$ has now been observed by two groups.^{30,31} The more recent measurement³⁰ has over two hundred events and exhibits a clear signal. Unfortunately, the only asymmetry measurement³⁰ has a large statistical uncertainty and is only able to provide weak evidence for the sign.

For the Ξ^0 decays the two modes, $\Xi^0 \rightarrow \Lambda^0 \gamma$ and $\Xi^0 \rightarrow \Sigma^0 \gamma$ have both been observed.³²⁻³⁴ The limited statistics (≈ 100 events) in each final state severely limit the precision of the asymmetry and branching fraction measurements. It is very important that the measurements of these branching fractions and asymmetries be repeated with higher precision.

None of the Ω^- radiative decays have been observed although a recent experiment³⁵ has reduced the limit on the $\Omega^- \rightarrow \Xi^- \gamma$ branching fraction significantly.

3. Hara's Theorem

Weak radiative hyperon decays (WRHD) are a puzzle because of Hara's theorem⁴² which states that the parity violating amplitude of the decay $\Sigma^+ \rightarrow p\gamma$ (as well as that of $\Xi^- \rightarrow \Sigma^- \gamma$) should vanish in the limit of SU(3) flavor symmetry. This theorem is crucial to understanding the theoretical implications for the weak radiative hyperon decays. We thus start the theoretical part of this review with the presentation of Hara's theorem.

In his original paper Hara⁴² assumed octet dominance of the nonleptonic weak interactions. This assumption is experimentally well verified in all strangeness changing weak decays involving hadrons. It states that the weak interaction Hamiltonian transforms like a member of the octet of flavor SU(3). Contributions from other representations (i.e. the 27-plet) contained in the product $3 \otimes 3 \otimes \bar{3} \otimes \bar{3}$ (describing possible SU(3) transformation properties of the Fermi interactions of four quarks) are assumed negligible. Subsequently, proofs of Hara's theorem have been given by Lo⁴³ and Gourdin.⁴⁴ Insightful comments have also been made by others.^{45,46} In the formulation of Gourdin, octet dominance was not used and the requirement of SU(3) symmetry was replaced by the weaker requirement of U-spin symmetry (basically, simple interchange of s and d quarks). Our approach below is similar to that of Gourdin. Later, in Section 6 we shall place Hara's theorem in a more elaborate theoretical framework.

3.1. Gauge invariance and U-spin arguments

Let us start our discussion by writing the most general parity violating coupling of photon to hadrons in the standard hadron-level language:

$$\bar{\psi}_1 \left[\gamma_\mu F_1(q^2) + q_\mu F_2(q^2) + i\sigma_{\mu\nu} q^\nu F_3(q^2) \right] \gamma_5 \psi_2 A^\mu. \quad (1)$$

Invariance under the gauge transformation

$$A^\mu \rightarrow A^\mu + q^\mu \chi \quad (2)$$

requires the vanishing of the additional term

$$\bar{\psi}_1 \left[q F_1 + q^2 F_2 \right] \gamma_5 \psi_2 \chi \quad (3)$$

generated by this transformation.

Consequently (as required also by current conservation), we must have

$$\bar{\psi}_1 \left[(m_1 + m_2) F_1 + q^2 F_2 \right] \gamma_5 \psi_2 = 0. \quad (4)$$

From (4) it follows that

$$F_1 = -\frac{q^2}{m_1 + m_2} F_2. \quad (5)$$

Since F_2 cannot have a pole at $q^2 = 0$ (no massless hadrons exist), F_1 must vanish at $q^2 = 0$, i.e., for real photons.

For real photons ($q^2 = q^\mu \cdot \varepsilon_\mu = 0$), only the third term, $F_3(0)$, in (1) may be nonvanishing. Since weak radiative hyperon decays are CP-conserving processes, we must deduce what restrictions the requirement of CP-invariance imposes upon this term. Under the operations of charge conjugation we have

$$\bar{\psi}_1 i\sigma_{\mu\nu} \gamma_5 \psi_2 q^\mu \xrightarrow{C} -\bar{\psi}_2 i\sigma_{\mu\nu} \gamma_5 \psi_1 q^\mu \quad (6)$$

corresponding to C-parity equal to -1 for the diagonal term

$$\bar{\psi}_1 i\sigma_{\mu\nu} \gamma_5 \psi_1 q^\mu \quad (7)$$

describing the situation when the incoming and outgoing baryons are identical ($2 \rightarrow 1$). Since the parity of expression (7) is +1, it cannot be coupled to the photon A^ν ($C_\gamma = P_\gamma = -1$) if CP is to be conserved.

In general, however, the incoming and outgoing particles are not identical, as in (1), and one can write an expression that is *antisymmetric* under the interchange of particles labels ($1 \nleftrightarrow 2$) in the initial (and final) state

$$\bar{\psi}_1 i\sigma_{\mu\nu} \gamma_5 \psi_2 q^\mu - \bar{\psi}_2 i\sigma_{\mu\nu} \gamma_5 \psi_1 q^\mu \quad (8)$$

and which goes into itself (with + sign) under the operation (6) of charge conjugation. Thus, expression (8) has *even* C-parity and, consequently, a coupling of the form

$$\left[\bar{\psi}_1 i\sigma_{\mu\nu} \gamma_5 \psi_2 - \bar{\psi}_2 i\sigma_{\mu\nu} \gamma_5 \psi_1 \right] q^\mu A^\nu \quad (9)$$

is permitted by CP-conservation.

For $1 \rightarrow p, 2 \rightarrow \Sigma^+$ we get the term considered by Hara:

$$\left[\bar{\psi}_p i\sigma_{\mu\nu} \gamma_5 \psi_{\Sigma^+} - \bar{\psi}_{\Sigma^+} i\sigma_{\mu\nu} \gamma_5 \psi_p \right] q^\mu A^\nu \quad (10)$$

as the only nonvanishing parity violating $\Sigma^+ p \gamma$ coupling permitted in the standard hadron level language.

Hara's theorem immediately follows from (10) as explained below. Indeed, since the weak $\Delta S = 1$ Hamiltonian is symmetric under the $s \rightleftharpoons d$ interchange one concludes that only the $s \rightleftharpoons d$ symmetric part of (10) may be non zero. However, $s \rightleftharpoons d$ corresponds to $\Sigma^+(uus) \rightleftharpoons p(uud)$, and under the $\Sigma^+ \rightleftharpoons p$ interchange, expression (10) is *anti*-symmetric. Consequently, the $s \rightleftharpoons d$ symmetric part of (10) is zero. Thus, in a U-spin symmetric world the $\Sigma^+ \rightarrow p \gamma$ parity violating amplitude should vanish. Similar considerations apply to the $\Xi^- \rightarrow \Sigma^- \gamma$ process since, under the $s \rightleftharpoons d$ interchange, $\Xi^-(ssd) \rightleftharpoons \Sigma^-(dds)$.

3.2. Abandoning exact $SU(3)$

In the real world, the strange quark is heavier than the down quark. Consequently, with U-spin symmetry broken, nonvanishing parity violating amplitudes (and therefore also asymmetries) are expected for the $\Sigma^+ \rightarrow p \gamma$ and $\Xi^- \rightarrow \Sigma^- \gamma$ processes.

This situation has been discussed by Vasanti.⁴⁷ To get a prediction for the sign of the resulting asymmetry let us consider his argument for the effective $s \rightarrow d \gamma$ transition. This transition is described by

$$M \propto \bar{d} \sigma_{\mu\nu} (a + b \gamma_5) s q^\mu A^\nu. \quad (11)$$

In Eq. (11) a and b depend on the masses m_s, m_d and b must vanish for $m_s = m_d$ as required by Hara's theorem.

Since the theory is invariant under the following transformations of fields and masses:

$$\begin{aligned}
q &\rightarrow -\gamma_5 q \\
\bar{q} &\rightarrow \bar{q} \gamma_5 \\
m_q &\rightarrow -m_q
\end{aligned} \tag{12}$$

corresponding to

$$\begin{aligned}
m_q \bar{q} q &\rightarrow (-m_q) \bar{q} \gamma_5 (-\gamma_5 q) = m_q \bar{q} q \\
\bar{q}' \gamma_\mu (1 - \gamma_5) q &\rightarrow \bar{q}' \gamma_\mu (1 - \gamma_5) (-\gamma_5 q) = \bar{q}' \gamma_\mu (1 - \gamma_5) q
\end{aligned}$$

etc.

and (12) holds separately for each flavor we may perform transformation (12) in Eq. (11) for the strange quark *only*. Assuming for the moment that a and b are odd in quark masses:

$$\begin{aligned}
a &= \varsigma m_d + \beta m_s \\
b &= \gamma m_d + \delta m_s
\end{aligned} \tag{13}$$

(and $\varsigma, \beta, \gamma, \delta$ are even)

we obtain then

$$\begin{aligned}
&\bar{d} \sigma_{\mu\nu} [(\varsigma m_d + \beta m_s) + (\gamma m_d + \delta m_s) \gamma_5] s \rightarrow \\
&\rightarrow \bar{d} \sigma_{\mu\nu} [-\gamma m_d + \delta m_s + (-\varsigma m_d + \beta m_s) \gamma_5] s.
\end{aligned} \tag{14}$$

Invariance under (12) requires then $\varsigma = -\gamma, \beta = \delta$ and Hara's theorem itself (i.e., vanishing of b for $m_s = m_d$) fixes $\beta = \varsigma$.

As far as the terms even in quark masses are concerned, one can similarly show that they must vanish. To this end one has to consider separately two transformations: $s \rightarrow -\gamma_5 s$, $m_s \rightarrow -m_s$ and $\bar{d} \rightarrow \bar{d} \gamma_5$, $m_d \rightarrow -m_d$.

Thus, from (14) and (11) we obtain

$$M \propto \bar{d} \sigma_{\mu\nu} \left(1 + \frac{m_s - m_d}{m_s + m_d} \gamma_5 \right) s q^\mu A^\nu. \tag{15}$$

From (15) it follows that the asymmetry parameter is positive:

$$\alpha = \frac{m_s^2 - m_d^2}{m_s^2 + m_d^2} \tag{16}$$

and close to +1 if current quark masses are used ($m_s \gg m_d$). If, on the other hand, one uses constituent quark masses ($m_s \approx 500$ MeV, $m_d \approx 330$ MeV) one gets α around +0.4 to +0.5.

One might hope that a similar argument may be applied to all hadron level transitions $B_1 \rightarrow B_2 \gamma$ when baryons B_1, B_2 are members of a U-spin doublet (as are s and d in (11)). That is, one would expect positive asymmetries for the $\Sigma^+ \rightarrow p \gamma$ and $\Xi^- \rightarrow \Sigma^- \gamma$ decays. As will be discussed at length in this review this expectation is not confirmed when one uses the quark model prescription for the structure of baryons. Yet, if single-quark transitions are dominant, the argument of Vasanti⁴⁷ is valid and leads to positive asymmetries for *all* weak radiative decays. If these transitions are not dominant, the above arguments still apply to the $\Xi^- \rightarrow \Sigma^- \gamma$ decay since single-quark transitions are the only ones that may contribute to this decay (Section 7).

3.3. The controversy

It came, therefore, as a great surprise^{48,49} when the first measurements^{24,25} indicated a *large negative* asymmetry in the $\Sigma^+ \rightarrow p \gamma$ decay. As discussed in Section 2 the most recent high statistics experiment performed at Fermilab⁸ confirms these findings and leaves no doubts as to the sign and size of the $\Sigma^+ \rightarrow p \gamma$ asymmetry:

$$\alpha(\Sigma^+ \rightarrow p \gamma) = -0.72 \pm 0.086 \pm 0.045 \quad (17)$$

where the quoted errors are statistical and systematic respectively. Thus, standard hadron-level arguments appear to be at gross variance with experiment.

The theoretical situation became muddled in 1983 when Kamal and Riazuddin⁵⁰ (KR) reconsidered the question within the framework of the quark model. The astonishing result of their simple, explicitly gauge-invariant calculation was that in the quark model, Hara's theorem is not satisfied in the SU(3) limit. Since the remaining assumptions upon which this theorem rests seem to be unshakable, their result has been considered by some workers as revealing a kind of pathology of the quark model.

Others, nonetheless, tried to find a place for it in the existing hadron-level formalism. We come back to the KR paper in Section 7 where we discuss if (and how) it is possible to fit this paper into the existing standard hadron-level theoretical framework of Section 6 as well as which of the assumptions of Hara's theorem appears to conflict with the quark model.

A resolution of the problem has been proposed⁵¹ but may be regarded by some as itself controversial. It is therefore of paramount importance to have a sound experimental input against which theoretical ideas may be tested. We shall review the actual status of our experimental knowledge on weak radiative hyperon decays in Section 5. Before embarking on a tour of the experimental side of the studies of weak radiative hyperon decays, in the next brief section we shall present lower bounds on the WRHD branching fractions. These bounds are imposed by unitarity and therefore they are very reliable.

4. Unitarity Bounds

Presentation and discussion of the predictions of specific models of WRHD will be given in Sections 7-9. Here we gather the most important and essentially model-independent lower bounds on the branching fractions of WRHD, that follow from unitarity. These bounds result from the nonvanishing of the contribution of πB intermediate states as shown in Fig. 4.1

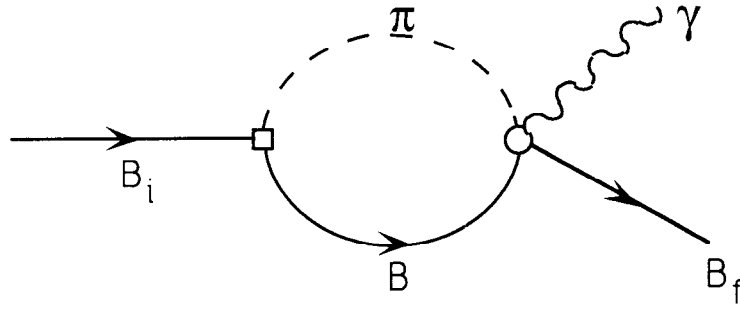


Fig. 4.1. Unitarity-induced contribution of the πB intermediate state to the WRHD $B_i \rightarrow B_f \gamma$ (\square -weak nonleptonic decay; \circ -pion photoproduction).

The first estimate of this contribution has been made by Zakharov and Kaidalov.⁵² In their paper they considered $\Sigma^+ \rightarrow p\gamma$, $\Lambda \rightarrow n\gamma$ and $\Xi^- \rightarrow \Sigma^-\gamma$ decays.

For the $\Sigma^+ \rightarrow p\gamma$ decay, $\text{Im } M(\Sigma^+ \rightarrow p\gamma)$ can be expressed in terms of the amplitudes of the $\Sigma \rightarrow N\pi$ nonleptonic decays and of those of pion photoproduction on nucleons ($\gamma p \rightarrow \pi^+ n$). Using the results of a phase-shift analysis of the photoproduction of pions on protons Zakharov and Kaidalov⁵² estimated that the branching fraction R for the $\Sigma^+ \rightarrow p\gamma$ decay satisfies

$$R(\Sigma^+ \rightarrow p\gamma) \geq (0.69 \pm 0.40) \cdot 10^{-4}. \quad (1)$$

The above number corresponds to case (1) of Zakharov and Kaidalov (i.e., to the domination of the p-wave in the decay $\Sigma^+ \rightarrow n\pi^+$, as it has been experimentally determined after their publication). For the $\Lambda \rightarrow n\gamma$ and $\Xi^- \rightarrow \Sigma^-\gamma$ decays the necessary experimental input in the form of the relevant phase-shift analyses was not available. Using perturbation theory estimates of the s-wave pion photoproduction amplitudes (the s-wave constitutes the dominant amplitude in relevant nonleptonic decays), Zakharov and Kaidalov concluded that the following lower bounds for the $\Lambda \rightarrow n\gamma$ and $\Xi^- \rightarrow \Sigma^-\gamma$ branching fractions should hold:

$$R(\Lambda \rightarrow n\gamma) \geq 0.83 \times 10^{-3} \quad (2)$$

$$R(\Xi^- \rightarrow \Sigma^- \gamma) \geq 0.13 \times 10^{-3}. \quad (3)$$

The same number for the lower bound on the $\Lambda \rightarrow n\gamma$ branching fraction has been independently obtained by Farrar.⁵³ Adding an estimate of the real part she concluded that

$$R(\Lambda \rightarrow n\gamma) \approx (1.9 \pm 0.8) \times 10^{-3} \quad (4)$$

and that the corresponding asymmetry is likely to be positive.

For the $\Sigma^+ \rightarrow p\gamma$ lower bound Farrar found a value smaller by an order of magnitude from the one given by Zakharov and Kaidalov⁵² in Eq.1.

An independent estimate of the branching fraction for the $\Xi^- \rightarrow \Sigma^- \gamma$ decay has been made by Kogan and Shifman.⁵⁴ Their calculation of the diagram of Fig. 4.1 gives

$$R(\Xi^- \rightarrow \Sigma^- \gamma) \geq 0.10 \times 10^{-3}. \quad (5)$$

Taking the real part into account they estimate

$$R(\Xi^- \rightarrow \Sigma^- \gamma) \geq 0.17 \times 10^{-3}. \quad (6)$$

Finally, a thorough study of the contribution of πN intermediate states to the weak radiative decays of Σ and Λ hyperons has been carried out by Reid and Trofimenkoff.^{55,56} Their approach contains some technical and phenomenological improvements over that of Farrar.⁵³ Reid and Trofimenkoff⁵⁵ also contain references to earlier papers on the contribution of the πB intermediate states.

We have gathered all these lower bounds determined by the imaginary parts of the amplitudes corresponding to Fig. 4.1 and the full predictions (which include, fairly uncertain, estimates of real parts) in Table 4.1.

Table 4.1 Comparison of estimates of πB contributions to the branching fractions of WRHD. (in units of 10^{-3})

	Zakharov ⁵²	Farrar ⁵³		Kogan ⁵⁴		Reid ^{55,56}
Process	lower bound	lower bound	full estimate	lower bound	full estimate	full estimate
$\Sigma^+ \rightarrow p\gamma$	0.07±0.04	0.007	0.3±1.2			0.77 ^{+1.29} _{-0.49}
$\Lambda \rightarrow n\gamma$	0.83	0.85	1.9±0.8			1.20 ^{+0.46} _{-0.04}
$\Xi^- \rightarrow \Sigma^- \gamma$	0.13			0.10	0.17	
$\Omega^- \rightarrow \Xi^- \gamma$				0.008	0.01	

5. Specific Measurements and Techniques

5.1 $\Sigma^+ \rightarrow p\gamma$

Measured for the first time twenty five years ago, the large negative asymmetry in this reaction spurred further work in WRHDs. Figure 5.1 shows the history of this asymmetry measurement. In these plots we have combined in quadrature the statistical and systematic uncertainties for each of the measurements.

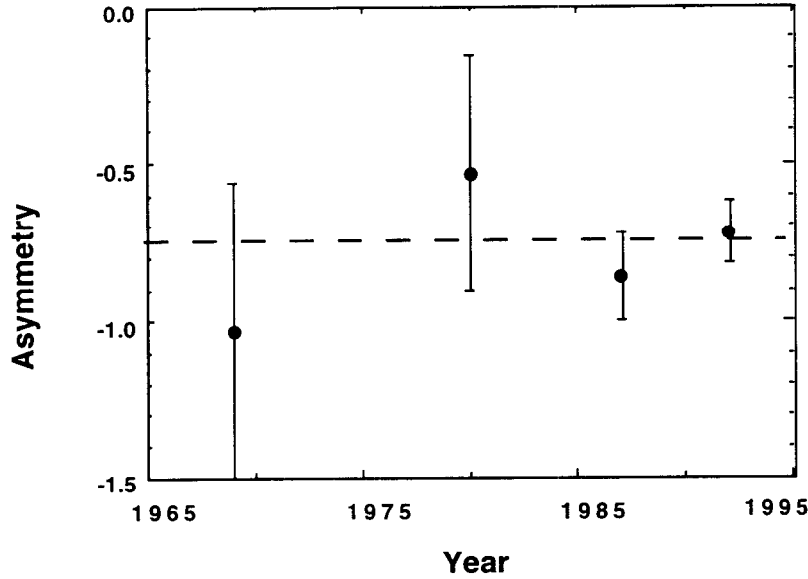


Figure 5.1 History of measurement of $\Sigma^+ \rightarrow p\gamma$ asymmetry parameter

From Fig. 5.1 we see a steady reduction in the uncertainties of the individual measurements. Combining these measurements we find for the $\Sigma^+ \rightarrow p\gamma$ asymmetry parameter, $\alpha = -0.76 \pm 0.08$. This is shown on Fig 5.1 by the dashed line. Crucial to these experiments is the ability to produce a Σ^+ with well known and controllable polarization. The primary measurement is of the decay asymmetry which is the product of the polarization and the intrinsic asymmetry parameter, α . Knowledge of the polarization comes from the measurement of a decay which has a known α parameter in the same beam or from a reliance on some other method of the determination of the polarization. Knowledge of the production polarization through known phase shifts has provided this for the low energy experiments.

These measurements utilize a variety of techniques to produce the polarized Σ^+ needed for asymmetry measurement which is illustrated in Table 5.1. The fact that the polarizations are derived from different reactions and are of differing magnitudes but that

the experiments still give consistent values of α lead one to the inescapable conclusion that α is large and negative in the decay $\Sigma^+ \rightarrow p\gamma$.

Table 5.1 Properties of $\Sigma^+ \rightarrow p\gamma$ asymmetry experiments

Experiment	Laboratory	Reaction	Σ^+ Momentum GeV/c	Polarization %
Foucher ⁸	Fermilab	$p\text{ Cu} \rightarrow X\ \Sigma^+$	375.	12.
Kobayashi ³⁸	KEK	$\pi^+ p \rightarrow K^+ \Sigma^+$	1.7	87.
Manz ²⁵	CERN	$\pi^- p \rightarrow K^- \Sigma^+$	0.42-0.50	≈ 10 -90
Gershwin ²⁴	LBL	$K^- p \rightarrow \pi^- \Sigma^+$	0.5	40.

The branching fraction measurements are plotted in Fig. 5.2 and give a similarly consistent picture. Again these experiments use different techniques and have differing systematic uncertainties. Their weighted mean and standard deviation is

$$(\Sigma^+ \rightarrow p\gamma)/(\Sigma^+ \rightarrow \text{all}) = (1.23 \pm 0.06) \times 10^{-3}$$

and is represented by a dashed line in Fig. 5.2.

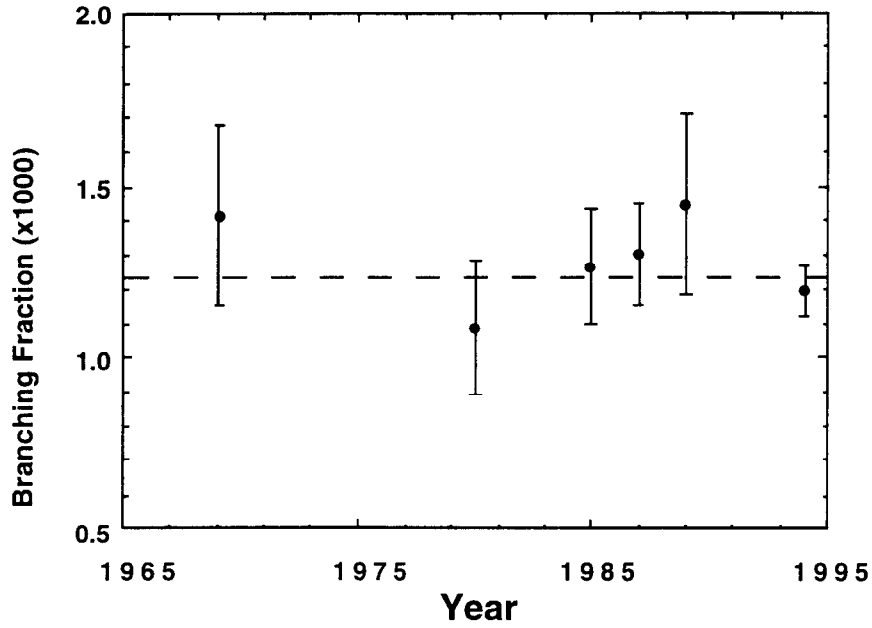


Figure 5.2 History of measurement of $\Sigma^+ \rightarrow p\gamma$ branching fraction

Needed in these experiments is both the ability to produce sufficient samples of polarized hyperons as well as careful control of systematic uncertainties. We illustrate how this is done by looking in some detail at one of these experiments.

The experiment of Foucher et. al.⁸ is shown in Fig. 5.3. In this classic high energy charged hyperon beam experiment, the Σ^+ are produced by 800 GeV protons incident on a small Cu target at the entrance of a large "hyperon" magnet. The latter serves as a magnetic channel selecting particles within a narrow momentum and angle range thus defining the transverse momentum, p_t , and Feynman x , x_f , of the produced hyperons. Reversing the sign of the targeting angle reverses the sign of the hyperon polarization. Since this can be done by changing currents in magnets upstream of the "hyperon" magnet, the resolutions and backgrounds in the spectrometers are not affected. This is a powerful technique for controlling systematic uncertainties.

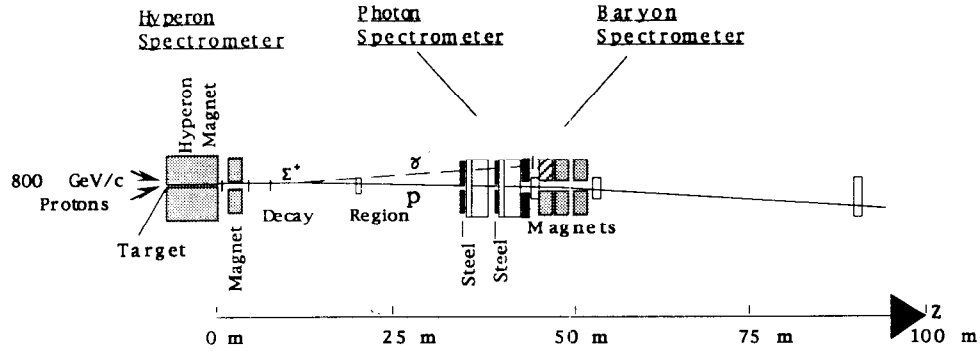


Fig. 5.3 $\Sigma^+ \rightarrow p\gamma$ Apparatus of Foucher et. al.⁸

The charged beam had a mean momentum of 375 GeV/c and provided a large flux ($\approx 2000 \Sigma^+$ per second) of Σ^+ at the decay region indicated in Figure 5.3. The momentum and direction of the beam particles were measured by the magnets and detectors of the hyperon spectrometer. The decay products of the Σ^+ were measured by the photon and baryon spectrometers.

High spatial resolution detectors in the hyperon and baryon spectrometers of Fig. 5.3 allowed excellent mass resolution. The required trigger was simple in that it only required the conversion of a neutral photon into a charged electromagnetic shower in a set of steel plates. This means that Σ^+ decaying through the $\Sigma^+ \rightarrow p\gamma$ were recorded at the same time as $\Sigma^+ \rightarrow p\pi^0$ decays, thus providing a measurement of the beam polarization from the well known decay properties of the $\Sigma^+ \rightarrow p\pi^0$. Fig. 5.4 shows a mass squared distribution (M_X^2) of the missing neutral particle (X^0) for the hypothesis $\Sigma^+ \rightarrow pX^0$ where we assume the hyperon track is a Σ^+ and the baryon track is a proton.

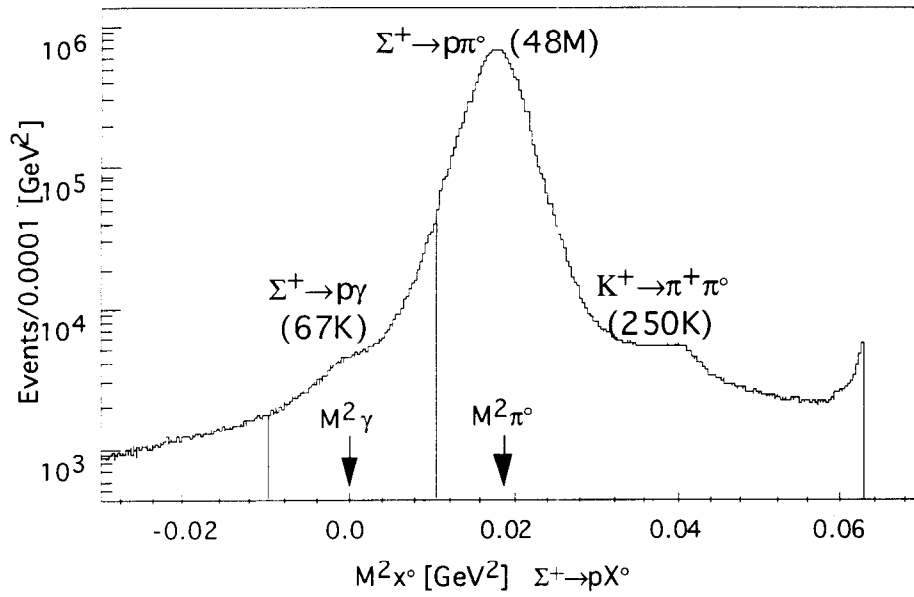


Fig. 5.4 Event distributions of the mass squared of the missing neutral particle (X^0) for the hypothesis $\Sigma^+ \rightarrow pX^0$

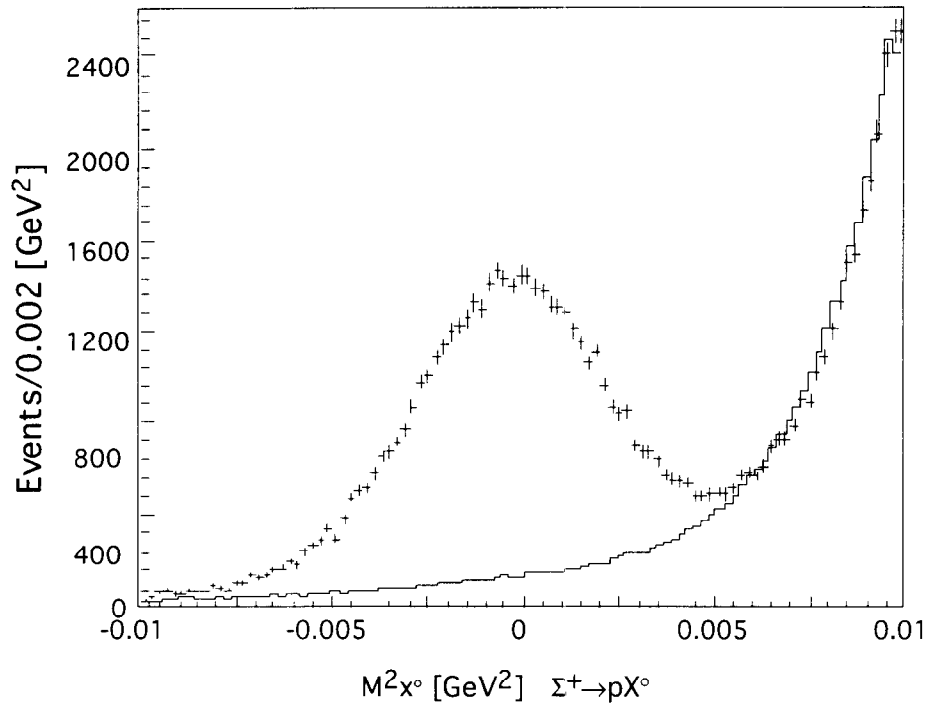


Fig. 5.5 Same as Fig. 5.4 after selection criteria are imposed. Note that one can estimate the background from the $\Sigma^+ \rightarrow pX^0$ peak.

Note the size of the event sample, the small shoulder corresponding to the radiative decay, and the peak corresponding to the decay of beam kaons. Imposition of selection criteria on the energy and angle of the neutral particle⁸ results in the event distribution of Fig. 5.5. Here the radiative decays are clearly seen above a relatively small background. The larger event sample and the ability to change the direction of polarization allowed this experiment to compete favorably with Kobayashi et. al.³⁸ even though their Σ^+ polarization was much larger as indicated in Table 5.1.

The measurements of Kobayashi et. al.³⁸ and Foucher et.al.⁸ used very different experimental techniques. Not only were their Σ^+ produced with different energies and polarizations, but also different methods of identifying the radiative decays were employed. Yet the fact that both experiments give similar and unambiguous results as shown in Figures 5.1 and 5.2 should reassure the reader that there are no hidden sources of systematic uncertainty. The $\Sigma^+ \rightarrow p \gamma$ branching fraction and asymmetry parameter are the most precisely measured of any of the radiative decays. There is no way of escaping the fact that the asymmetry is *large* and *negative*. Statistically, it is almost *ten standard deviations from zero*.

By reversing the currents in the magnets shown in the experiment of Fig. 5.5, a measurement^{16,57} has been made of a WRHD of an antibaryon, $\bar{\Sigma}^- \rightarrow \bar{p} \gamma$. Its measured decay parameters are consistent with CPT invariance.

5.2 $\Lambda^0 \rightarrow n \gamma$

This decay presents special problems to the experimenter since both the initial and final states are neutral. Although the asymmetry has not been measured so far, two measurements have been made of the branching fraction.^{27,29} The first measurement²⁹ utilized Λ^0 from the decay $\Xi^- \rightarrow \Lambda^0 \pi^-$ in the CERN charged hyperon beam. The momentum and the direction of the Λ^0 were determined from the momentum and direction of the Ξ^- and π^- . Although the Λ^0 resulting from the Ξ^- decay are polarized, the small event sample from this experiment (31 events) allowed for a measurement of the branching fraction only.

The second experiment^{3,27,28} utilized a very different technique. A stopping beam of K^- produces Λ^0 s through the reaction $K^- p \rightarrow \Lambda^0 \pi^0$. Measurement of the energy and direction of the two photons from the π^0 decay fixes the kinematics of the Λ^0 . In this case the Λ^0 is unpolarized. As can be seen from Table 2.1 the two experiments are in poor agreement differing by about 2σ . High intensity charged hyperon beams are available at Fermilab which could produce large fluxes of polarized Λ^0 from Ξ^- decays. Definitive measurements of both the branching fraction and asymmetry could be made at Fermilab.

5.3 $\Xi^0 \rightarrow \Lambda^0 \gamma$ and $\Xi^0 \rightarrow \Sigma^0 \gamma$

The identification of these all neutral topologies relies on the observation of the decay $\Lambda^0 \rightarrow p\pi^-$ for the $\Xi^0 \rightarrow \Lambda^0 \gamma$ or the electromagnetic decay $\Sigma^0 \rightarrow \Lambda^0 \gamma$ for the $\Xi^0 \rightarrow \Sigma^0 \gamma$. Both of these Ξ^0 WRHDs have been measured^{32,33} in Proton Center neutral beams at Fermilab. The geometry of these experiments was similar and is illustrated in Fig. 5.6. In each case a high energy proton beam impinging on a small target. A large high field magnet served to deflect charged particles and produce a collimated neutral beam containing Ξ^0 as well as more copious amounts of Λ^0 , K^0 , and neutrons. The Ξ^0 component can be identified because it is the only source of Λ^0 which do not originate in the target. (Since the Σ^0 lifetime is very short, Λ^0 produced by its decay appear to come from the target.) Because the Ξ^0 were inclusively produced, one does not have direct measurement of their momenta. However, from the reconstruction of the direction and momenta of the Λ^0 from its decay $\Lambda^0 \rightarrow p\pi^-$, one can combine this with photons in the same event to determine the Ξ^0 direction and momentum.

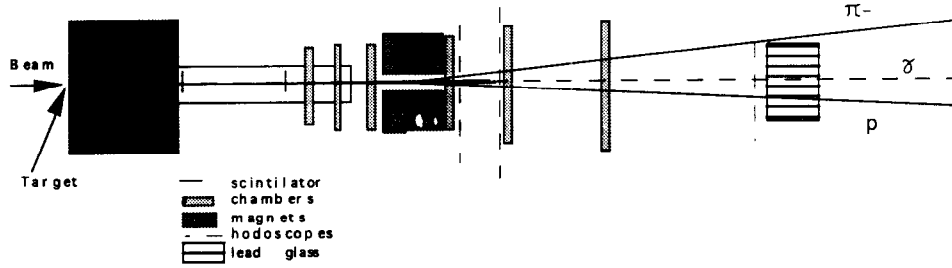


Fig. 5.6 Simplified version of the apparatus of Teige et al.³³

We note that these experiments were done as subsidiary measurements in existing experimental configurations and each contained less than 100 events. These pioneering measurements demonstrated the versatility of high energy neutral hyperon beams in extracting the parameters of the Ξ^0 WRHDs. Enhanced statistical precision is clearly needed, however. This is particularly important for the determination of the asymmetry parameters since at this time one is not even sure of their signs.

The Fermilab neutral kaon facility now under construction may offer the best possibility for new information on the Ξ^0 WRHDs.⁵⁸ This experiment has as its primary goal the measurement of CP violating parameters in the kaon system and has excellent photon detection capabilities. Utilization of the Ξ^0 component of this beam has the capabilities of increasing the statistics of the Ξ^0 WRHDs by one to two orders of magnitude.

5.4 $\Xi^- \rightarrow \Sigma^- \gamma$

This decay presents experimental challenges because of its small branching ratio ($\approx 10^{-4}$), the small polarization of the Ξ^- ($\approx 10\%$), and the need to identify the Σ^- either directly or through its major decay mode $\Sigma^- \rightarrow n\pi^-$ in order to suppress backgrounds. The branching fraction was first measured in the CERN hyperon beam³¹ with a sample of 11 events. More recently the Fermilab group³⁰ with about 200 events was able to improve on its value as well as present weak evidence that the asymmetry parameter is positive. The measurement of the asymmetry parameter is of particular importance since this is the most accessible WRHD that cannot proceed by a two quark diagram (Fig. 7.1). Consequently, an improved measurement would help shed light on the other processes.

5.5 $\Omega^- \rightarrow \Xi^- \gamma$ and $\Omega^- \rightarrow \Xi^*(1530) \gamma$

Neither of these decays have been seen. The considerably lower fluxes of Ω^- in hyperon beams (compared to Σ^- and Ξ^-) coupled with the observation that Ω^- are produced unpolarized^{59,60} make these branching fractions and asymmetry parameters particularly difficult to measure. Tertiary beams of polarized Ω^- have been produced and used to measure the Ω^- magnetic moment.⁶¹ However since they involve using polarized hyperon interactions to produce polarized Ω^- in a spin transfer mechanism, there is a further reduction in Ω^- beam rate. While a new experiment might be expected to push the $\Omega^- \rightarrow \Xi^- \gamma$ branching fraction to a level where it might be seen, a measurement of the asymmetry is not on the near horizon.

6. General Theoretical Framework

Great interest in weak radiative hyperon decays was stimulated both by the apparent disagreement between Hara's theorem and experiment and by the argument that nonetheless these hyperon decays should appear simpler and more susceptible to theoretical description than the nonleptonic ones. In the latter case the presence of two strongly interacting particles in the final state requires consideration of all complications due to final-state strong interactions while in WRHD one of the two outgoing particles is a strong-interaction-blind photon. Thus, final-state strong interactions appear to be absent in WRHD whose description may consequently be expected to be less dependent upon unknown details of strong interaction dynamics.

However, as the problems with Hara's theorem indicate, this expectation is misleading. Proper description of weak radiative hyperon decays is, most probably, at least as difficult as that of nonleptonic ones where there is no consensus as to the relative size (and sometimes also sign) of the contributions from various physical mechanisms. The standard general theoretical framework used in the description of nonleptonic decays is not disputed, however. Most attempts at a description of WRHD fit into a similar

standard framework. These two frameworks constitute two parts of a single theoretical scheme that unites weak couplings of pseudoscalar and vector particles to baryons. This general theoretical scheme has been known for years.⁶² It has been reviewed recently anew in an updated form⁶³⁻⁶⁵ which takes into account the development of the quark model in the intervening years. In this section, we describe this general scheme of the weak couplings of pseudoscalar and vector particles to baryons. We shall consider here the requirements imposed by the conditions of gauge invariance only very briefly. Their further discussion is shifted to appropriate sections of this review where we show how calculations of various papers fit into the general scheme presented here.

Let us therefore consider the couplings $B_i B_f M$ (where $B_{i(f)}$ denotes the initial (final) baryon and M is pseudoscalar (P) or vector (V) particle) in the presence of weak interactions.

In general, the weak interaction Hamiltonian may act in any one of the three legs of the $B_i B_f M$ coupling as shown in Fig. 6.1.

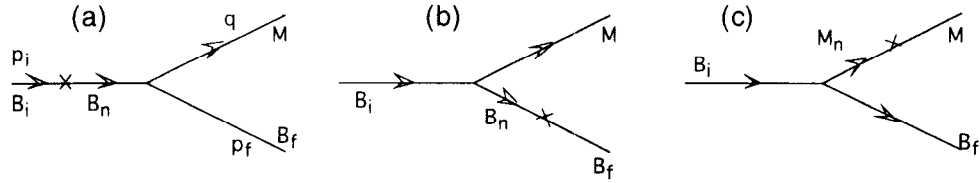


Fig. 6.1abc. Diagrams for the weak $B_i B_f M$ coupling.

The cross denotes the action of the weak Hamiltonian.

We postpone the discussion of the boson-leg contribution (c) for the moment and focus on diagrams (a) and (b). To stress similarities between the weak couplings of pseudoscalar and vector particles, we shall consider both of them alongside each other starting from a fairly extensive discussion of the troublesome parity violating amplitudes. This will be followed by a brief presentation of the standard approach to the parity conserving amplitudes.

6.1 The contribution of baryon poles

6.1.1 Parity violating amplitudes

Let us consider the action of the parity violating part $H^{p.v.}$ of the weak Hamiltonian in the baryon legs of Fig. 6.1. The intermediate states B_n may be the ground $B_n(\frac{1}{2}^+)$ and the excited $B_{n^*}(\frac{1}{2}^-)$, $B_{n^*}(\frac{1}{2}^+)$, ... baryon states. The Lee-Swift theorem⁶⁶ requires that in the SU(3) symmetry limit the matrix elements of $H^{p.v.}$ between the ground states

vanish. Therefore, the contribution of the intermediate ground states $B_n\left(\frac{1}{2}^+\right)$ is generally neglected. The dominant contribution is then expected to come from the excited $B_{n^*}\left(\frac{1}{2}^-\right)$ baryons.

6.1.1.1 Pseudoscalar particles – nonleptonic decays

General expressions for the parity-violating (s-wave) $B_i \rightarrow B_f M$ nonleptonic hyperon decay (NLHD) amplitudes are

$$\begin{aligned} M^{P.V.}\left(B_i \rightarrow B_f P\right) &= A \bar{u}_f u_i \\ M^{P.V.}\left(B_i \rightarrow B_f V\right) &= \varepsilon^{*\mu} \bar{u}_f \left[A_1 \gamma_\mu + A_2 q_\mu + A_3 i \sigma_{\mu\nu} q_\nu \right] \gamma^5 u_i \\ \left(\sigma_{\mu\nu} \right) &= \frac{i}{2} \left[\gamma_\mu \gamma_\nu - \gamma_\nu \gamma_\mu \right]. \end{aligned} \quad (1)$$

It is straightforward to show that for the pseudoscalar mesons, the excited $B_{n^*}\left(\frac{1}{2}^-\right)$ baryons contribute to the A amplitude as follows

$$A = \sum_{B_{n^*}\left(\frac{1}{2}^-\right)} \left[\frac{g_{B_f B_{n^*} P} b_{n^* i}}{m_i - m_{n^*}} + \frac{b_{fn^*} g_{B_{n^*} B_i P}}{m_f - m_{n^*}} \right] \quad (2)$$

where

$$\begin{aligned} \left\langle B_{n^*}\left(\frac{1}{2}^-\right) \right| H^{P.V.} \left| B_i\left(\frac{1}{2}^+\right) \right\rangle &= b_{n^* i} \bar{u}_{n^*} u_i \\ \left\langle B_f\left(\frac{1}{2}^+\right) \right| H^{P.V.} \left| B_{n^*}\left(\frac{1}{2}^-\right) \right\rangle &= b_{fn^*} \bar{u}_f u_{n^*} \end{aligned} \quad (3)$$

with $b_{in^*} = b_{n^* i}$ (from hermiticity and CP invariance). In Eq. 2. g_{BB^*P} (g_{B^*BP}) are strong (parity conserving) couplings of pseudoscalar mesons to the $\left(\frac{1}{2}^+, \frac{1}{2}^-\right)$ pair of baryons

$$\begin{aligned} M^{Strong}\left(B_i \rightarrow B_{n^*} P\right) &= g_{B_{n^*} B_i P} \bar{u}_{n^*} u_i \\ M^{Strong}\left(B_{n^*} \rightarrow B_f P\right) &= g_{B_f B_{n^*} P} \bar{u}_f u_{n^*}. \end{aligned} \quad (4)$$

The standard current algebra form⁶⁷ is obtained from (2) through the use of generalized Goldberger-Treiman relations^{65,68}

$$\begin{aligned} g_{B^*BP} &= \frac{\sqrt{2}}{f_P} (m_{B^*} - m_B) g_A^{B^*B} \\ &= g_{BB^*P} = \frac{\sqrt{2}}{f_P} (m_B - m_{B^*}) g_A^{BB^*} \end{aligned} \quad (5)$$

where f_P is the decay constant of the pseudoscalar meson P and $g_A^{B^*B} = -g_A^{BB^*}$ is the axial vector coupling constant.

In the soft meson limit ($q^\mu \rightarrow 0$, $m_i \rightarrow m_f$) the use of Eq. 5 reduces Eq. 2 to the standard commutator relation of the current algebra approximation A^{CA} to A :

$$\begin{aligned} A^{CA} &= \lim_{q \rightarrow 0} A = \frac{\sqrt{2}}{f_{Pa}} \sum_{B_n^* \left(\frac{1}{2}^- \right)} \left(g_{Aa}^{B_f B_n^*} b_{n^*i} - b_{fn^*} g_{Aa}^{B_n^* B_i} \right) \\ &= + \frac{\sqrt{2}}{f_{Pa}} \langle B_f | [Q_5^a, H^{P.v.}] | B_i \rangle \end{aligned} \quad (6)$$

where Q_5^a is the axial charge. Away from the soft meson limit, we have

$$A = A^{CA} + \frac{\sqrt{2}}{f_{Pa}} (m_f - m_i) \sum_{B_n^* \left(\frac{1}{2}^- \right)} \left[\frac{g_A^{B_f B_n^*} b_{n^*i}}{m_i - m_{n^*}} + \frac{b_{fn^*} g_A^{B_n^* B_i}}{m_f - m_{n^*}} \right] \quad (7)$$

where the second term describes this part of the contribution from the excited intermediate states $B_{n^*} \left(\frac{1}{2}^- \right)$ that vanishes in the $q^\mu \rightarrow 0$ ($m_i = m_f$) limit and therefore cannot be absorbed into the standard commutator term of current algebra. The advantage of current algebra approach over that of the pole model appears in the limit of exact SU(3), when the second term in Eq. 7 vanishes and, consequently, no information on the $\frac{1}{2}^-$ poles is needed.

For further discussions of the relationship of the general scheme to the quark model calculations we need to establish a connection (if any) between the above considerations and the quark model. That such a connection exists has been observed by Körner and Gudehus.⁶⁹ In 1979 Körner, Kramer, and Willrodt⁷⁰ proved that the soft meson approach and the quark model are totally equivalent in a group theoretical sense. The question has been discussed also by Desplanques, Donoghue, and Holstein.⁶⁴ We shall come to the questions of dynamics in the quark model after completing our presentation of the standard general scheme.

6.1.1.2 Vector particles – radiative decays

For the vector particles, we have two possible (vector and tensor) strong (parity-conserving) couplings of vector mesons to the $\left(\frac{1}{2}^+, \frac{1}{2}^-\right)$ pair of baryons: [with $\varepsilon^{*\mu} q_\mu = 0$].

$$\begin{aligned} M^{Strong}(B_i \rightarrow B_{n^*} V^\mu) &= \varepsilon^{*\mu} \bar{u}_{n^*} \left[g_{B_{n^*} B_i V} \gamma_\mu + f_{B_{n^*} B_i V} i \sigma_{\mu\nu} q_\nu \right] \gamma_5 u_i \\ M^{Strong}(B_{n^*} \rightarrow B_f V^\mu) &= \varepsilon^{*\mu} \bar{u}_f \left[g_{B_f B_{n^*} V} \gamma_\mu - f_{B_f B_{n^*} V} i \sigma_{\mu\nu} q_\nu \right] \gamma_5 u_{n^*} \end{aligned} \quad (8)$$

with

$$\begin{aligned} g_{B_{n^*} B_i V} &= g_{B_i B_{n^*} V} \\ f_{B_{n^*} B_i V} &= f_{B_i B_{n^*} V}. \end{aligned} \quad (9)$$

From Eq. 3 and 8 it follows that: (1) the contribution from the vector coupling g_{B^*BV} to the parity violating $B_i \rightarrow B_f V$ amplitude is

$$\sum_{B_{n^*} \left(\frac{1}{2}^+ \right)} \left[\frac{b_{fn^*} g_{B_{n^*} B_i V}}{m_f - m_{n^*}} + \frac{g_{B_f B_{n^*} V} b_{n^* i}}{m_i - m_{n^*}} \right] \varepsilon^{*\mu} \bar{u}_f \gamma_\mu \gamma_5 u_i \quad (10)$$

and thus it determines A_1 in Eq. 1 while, (2) the contribution from the tensor coupling f_{B^*BV} is

$$\sum_{B_{n^*} \left(\frac{1}{2}^+ \right)} \left[\frac{b_{fn^*} f_{B_{n^*} B_i V}}{m_f - m_{n^*}} - \frac{f_{B_f B_{n^*} V} b_{n^* i}}{m_i - m_{n^*}} \right] \varepsilon^{*\mu} \bar{u}_f i \sigma_{\mu\nu} q_\nu \gamma_5 u_i \quad (11)$$

and thus it determines A_3 in Eq. 1.

When the vector particle under consideration is a photon, standard application of the requirement of gauge invariance to the $g_{B^*B\gamma}$ and $f_{B^*B\gamma}$ couplings implies (as in the Section on Hara's theorem) that

$$g_{B^*B\gamma} = 0. \quad (12)$$

Only the contribution from the tensor coupling $f_{B^*B\gamma}$ survives then leading (through Eq. 11) to the standard gauge invariant form of the $B_i B_f \gamma$ parity violating coupling used in the derivation of Hara's theorem.

6.1.2 Parity conserving amplitudes

Let us now consider the parity conserving amplitudes. Since the matrix elements $\langle B_{n*}(\frac{1}{2}^-) | H^{p.c.} | B(\frac{1}{2}^+) \rangle$ vanish in the SU(3) limit (just as in the Lee-Swift theorem), only the ground $B_n(\frac{1}{2}^+)$ and the excited $B_{n*}(\frac{1}{2}^+)$ states may contribute significantly to the parity conserving amplitudes. In simple models the contribution from the ground states is assumed to be dominant. Consequently, with

$$\langle B_m(\frac{1}{2}^+) | H^{p.c.} | B_n(\frac{1}{2}^+) \rangle = a_{mn} \bar{u}_m u_n. \quad (13)$$

we have the following expressions for the parity conserving (p-wave) $B_i \rightarrow B_f M$ amplitudes.

$$M^{p.c.}(B_i \rightarrow B_f P) = \bar{u}_f \gamma_5 u_i \cdot \sum_{B_n(\frac{1}{2}^+)} \left[\frac{g_{B_f B_n} P^{ani}}{m_i - m_n} + \frac{a_{fn} g_{B_n B_i} P}{m_f - m_n} \right] \quad (14)$$

and

$$\begin{aligned} M^{p.c.}(B_i \rightarrow B_f V) &= \varepsilon^{*\mu} \bar{u}_f \gamma_\mu u_i \cdot \sum_{B_n(\frac{1}{2}^+)} \left[\frac{g_{B_f B_n} V^{ani}}{m_i - m_n} + \frac{a_{fn} g_{B_n B_i} V}{m_f - m_n} \right] \\ &+ \varepsilon^{*\mu} \bar{u}_f \gamma^\mu \sigma_{\mu\nu} q_\nu u_i \cdot \sum_{B_n(\frac{1}{2}^+)} \left[\frac{f_{B_f B_n} V^{ani}}{m_i - m_n} + \frac{a_{fn} g_{B_n B_i} V}{m_f - m_n} \right] \end{aligned} \quad (15)$$

where $g_{BBV}(f_{BBV})$ are vector (tensor) parts of the $B_i B_n V$ or $B_n B_f V$ coupling constants.

6.2 The quark model and QCD

As mentioned before, for the parity violating NLHD amplitudes the soft meson approximation and the quark model results were shown to be equivalent in a group-theoretical sense. Such an equivalence leaves plenty of room for the dynamics. The modern way of supplementing the quark model with the dynamics involves introduction of quantum chromodynamics and its subsequent treatment through the application of the operator-product expansion and the renormalization-group techniques.⁷¹

The effective operator employed to analyze $\Delta S = 1$ weak interactions has the form⁷²⁻⁷⁴

$$H_{\Delta S=1} = \frac{G_F \sin \theta_c \cos \theta_c}{2\sqrt{2}} \sum_i c_i O_i + h.c. \quad (16)$$

where the four-quark operators $\{O_i\}$ are the lowest-dimension operators appearing in the operator-product expansion and are defined by

$$\begin{aligned} O_1 &= H_A - H_B \\ O_2 &= H_A + H_B + 2H_C + 2H_D \\ O_3 &= H_A + H_B + 2H_C - 3H_D \\ O_4 &= H_A + H_B - H_C \\ O_5 &= \bar{d} \Gamma_L^\mu \lambda^A s \sum_Q \left(\bar{Q} \Gamma_{R\mu} \lambda^A Q \right) \\ O_6 &= \bar{d} \Gamma_L^\mu s \sum_Q \left(\bar{Q} \Gamma_{R\mu} Q \right) \end{aligned} \quad (17)$$

with

$$\begin{aligned} H_A &= \bar{d} \Gamma_L^\mu u \bar{u} \Gamma_{L\mu} s \\ H_B &= \bar{u} \Gamma_L^\mu u \bar{d} \Gamma_{L\mu} s \\ H_C &= \bar{d} \Gamma_L^\mu d \bar{d} \Gamma_{L\mu} s \\ H_D &= \bar{s} \Gamma_L^\mu s \bar{d} \Gamma_{L\mu} s \end{aligned} \quad (18)$$

and

$$\Gamma_L^\mu \equiv \gamma^\mu (1 + \gamma_5), \quad \Gamma_R^\mu \equiv \gamma^\mu (1 - \gamma_5) \quad (19)$$

The long-distance physics resides in the matrix elements of the O_i operators. The “penguin” operators O_5, O_6 (see Fig. 6.2.) have a $(V - A)(V + A)$ chiral structure whereas the remaining O_i operators are $(V - A)(V - A)$.

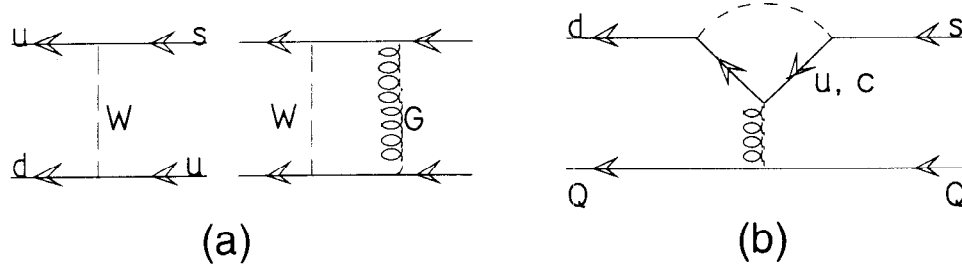


Fig. 6.2. Diagrams corresponding to the effective $\Delta S = 1$ Hamiltonian:
(a) nonpenguin (b) penguin.

Operators O_1, O_2, O_5 and O_6 transform like SU(3) octets and are $\Delta I = \frac{1}{2}$ operators. O_3 and O_4 are 27-plets carrying $\Delta I = \frac{1}{2}$ and $\Delta I = \frac{3}{2}$ respectively. The coefficients c_i contain the short-distance effects of hard gluons and are calculated by studying the QCD renormalization group equations. Without QCD evolution one has $c_1 = 1$, $c_2 = \frac{1}{5}$, $c_3 = \frac{2}{5}$, $c_4 = \frac{2}{3}$, $c_5 = c_6 = 0$. For the case under consideration a typical set⁷⁴⁻⁷⁶ of these coefficients is

$$\begin{aligned} c_1 &\sim 2.5 & c_2 &\sim 0.08 & c_3 &\sim 0.08 & c_4 &\sim 0.40 \\ c_5 &\sim -0.05 \rightarrow -0.1 & c_6 &\sim -0.01 \rightarrow -0.05. \end{aligned} \quad (20)$$

Thus, radiative QCD corrections result in the enhancement of the octet $\Delta I = \frac{1}{2}$ O_1 operator and the suppression of the $\Delta I = \frac{3}{2}$ O_4 operator.^{73,77} This dynamical argument goes some way towards the explanation of the $\Delta I = \frac{1}{2}$ rule. Furthermore, with penguin operators being flavor octet $\Delta I = \frac{1}{2}$ objects, a further enhancement of the $\Delta I = \frac{1}{2}$ amplitudes is predicted. The standard values of the penguin coefficients c_5, c_6 are small: they vanish in the limit of $m_c = m_u$ because of GIM cancellation. They are too small by a factor of order 5 to provide a satisfactory explanation of the $\Delta I = \frac{1}{2}$ rule.^{76,78}

In the baryon sector, however, this $\Delta I = \frac{1}{2}$ rule is readily explained as an automatic consequence of color symmetry. The relevant argument, known as the Pati-Woo theorem^{79,80} implies the vanishing of the matrix elements of the $\Delta I = \frac{3}{2}$ operator O_4 between the baryonic states. Actually, one can show⁷⁶ that

$$\langle B' | O_i | B \rangle = 0 \quad \text{for } i = 2, 3, 4. \quad (21)$$

Thus, the net effect of the QCD-enhancement factors is just to change the overall size of the Pati-Woo-allowed baryon-to-baryon weak matrix elements of diagrams (a) and (b) in Fig. 6.1. It *cannot* change such qualitative characteristics of quark model calculations as the violation of Hara's theorem in this model, that is the basis of the controversy regarding the WRHD. The QCD considerations of this section might,

however, be more important in the boson-leg diagrams (Fig. 6.1c) where the Pati-Woo theorem does not apply.

6.3 The boson-leg contribution

At the quark level the boson-leg contribution (Fig. 6.1c) is often identified with the factorizable amplitude. The factorization prescription corresponds to the insertion of the vacuum state between the quark bilinears of the 4-quark Fermi interaction. In the case of nonleptonic hyperon decays, upon invoking PCAC, the use of factorization prescription gives a contribution that vanishes in the SU(3) limit.⁸¹ At the hadron level the strength of the kaon-pole diagrams relevant in the parity conserving amplitudes is governed by the $K\pi$ transition matrix elements. It has been stressed^{63,76} that quark model estimates of $\langle \pi | H_{weak} | K \rangle$ involve substantial cancellations and cannot be reliably computed. Application of chiral Lagrangians to provide phenomenological estimates of these matrix elements indicates that kaon pole terms are small in comparison to the baryon pole terms.⁶³ For a thorough review of the meson sector relevant here see a recent paper by Cheng.⁷⁸ In other phenomenological studies of NLHD the kaon pole contribution is substantial, however.^{82,83} This disagreement constitutes just one example of the lack of general consensus concerning the relative magnitudes of various contributions in the nonleptonic hyperon decays. We shall discuss other such disagreements in the next section.

Since the decays of hyperons to other ground-state baryons and vector mesons are kinematically forbidden, we know even less about the boson-leg contribution for vector particles. Consequently, the contribution of this type of diagram in the weak radiative hyperon decays is often treated with the help of free parameters. Indeed, as Gilman and Wise⁷⁵ put it

“while sometimes disguised in the language of the operator-product expansion, much of the short-distance analysis boils down in the end to finding the local operators which correspond in a particular model to the amplitude for the transition of an s-quark to a d-quark plus photon”.

7. Phenomenology of the Standard Approach

7.1 Pole models

As it has been discussed in the previous section, the standard schemes for the description of the nonleptonic and weak radiative hyperon decays belong to the same general theoretical framework. Thus, it is quite plausible that our present phenomenological knowledge of NLHD might be useful in providing not only a background but also some important input needed for an understanding of WRHD. Accordingly, we must present first a brief overview of the present phenomenological situation in the NLHD sector.

7.1.1 Nonleptonic hyperon decays

As mentioned before, there is no consensus as to what are the relative sizes of various contributions to the NLHD amplitudes. Before we present the conflicting theoretical views, let us therefore recall the model-independent characteristics of these decays. These are given by SU(3) fits to the relevant experimental amplitudes, obtained as follows.

For the parity violating amplitudes, the soft-pion approximation (Eq. 6.6) can further be reduced through the use of the commutation relation

$$[Q_5^a, H^{P.V.}] = [Q^a, H^{P.C.}] \quad (1)$$

where Q^a is an SU(3) generator.

After working out the action of Q^a on the baryon states $(Q^a|B_i\rangle = |B_1\rangle, \langle B_f|Q^a = \langle B_2|)$ one finds that the current algebra approximation A^{CA} is given in terms of the matrix elements of the parity-conserving part $H^{P.C.}$ of the weak Hamiltonian between some baryon octet states B, B'

$$\langle B|H^{P.C.}|B'\rangle \quad (2)$$

The SU(3) parameterization of this matrix element is

$$\langle B|H^{P.C.}|B'\rangle = f\text{Tr}(S[B', B^+]) + d(S\{B', B^+\}) \quad (3)$$

where B', B on the right-hand side are standard 3×3 matrices corresponding to the baryons in question and $S = \lambda_6$ is the ($s \nleftrightarrow d$ symmetric) octet spurion representing the weak Hamiltonian. SU(3) fits to the s-wave amplitudes⁸⁴ give $f/d = -2.5$. Similar fits^{51,63,85-87} to the p-waves yield $f/d = -1.8$ to -1.9 . These experimental numbers still constitute a problem for the *valence* quark model (current algebra)⁸⁸ in which one obtains $f/d = -1$.

Existence of relatively good SU(3) fits to the NLHD amplitudes indicates that in these decays SU(3) is a fairly good approximate symmetry. Thus, the Lee-Swift theorem should be satisfied fairly well in the real world. Still, one may wonder how big the $\langle B|H^{P.V.}|B'\rangle$ matrix elements could be when SU(3) is weakly broken. Theoretical estimates of the ratios $\langle B|H^{P.V.}|B'\rangle/\langle B|H^{P.C.}|B'\rangle$ performed by Golowich and Holstein⁸⁹ in the context of the bag model indicate that they are of order of 1% in NLHD (5% in WRHD). As far as WRHD are concerned, the above considerations support, therefore, the assumption of the overall SU(3) symmetry used in the proof of Hara's theorem.

The origin of the discrepancy between the *valence* quark model and the experimental values for the f/d ratio has not been yet agreed upon. LeYaouanc et al. proposed⁹⁰ that the departure of the phenomenologically determined f/d ratio from its

valence quark model/current algebra value is due to a nonvanishing contribution of the second term in Eq. 6.7 (which vanishes for degenerate octet baryons). In explicit quark model calculations, they have found that this term is of the order of 50% and negative with respect to the commutator term. Using the pole model fit of Gronau⁸⁸ for the p-waves (which, when experimental baryon masses are used, needs $f_d \approx -1.18$) they were able to explain both the value of f_d observed in the s-wave amplitudes and the relative size of s-wave and p-wave amplitudes (the s:p ratio).

General theoretical scheme of the previous section admits, however, contributions from other intermediate states besides the $(56, 0^+) \frac{1}{2}^+$ and $(70, 1^-) \frac{1}{2}^-$ baryons discussed in LeYaouanc et. al.⁹⁰ A thorough study of the contributions from radially excited $(56, 0^+) \frac{1}{2}^+$ baryons as well as K^* and K mesons has been carried out by Bonvin.⁸² His calculations confirm general qualitative features of LeYaouanc et. al.⁹⁰ i.e., that the SU(3) symmetry breaking part of the contribution of $(70, 1^-) \frac{1}{2}^-$ is significant and interferes destructively with the commutator contribution, thus partially curing the problem of the s:p ratio. However, he also finds that the contributions from the meson-leg diagrams and the $(56, 0^+) \frac{1}{2}^+$ radially excited baryons are far from being negligible. As a result, his decomposition's of the amplitudes A and B into different contributions are totally different from those of LeYaouanc et. al.⁹⁰

Another approach for alleviating the f_d problem has been proposed by Donoghue and Golowich⁹¹ who considered the effects of quark sea on the soft-meson approximation A^{CA} . Both the QCD sea (corresponding to the *enhanced* penguin contribution)⁹¹ and the sea generated by unitarity on the hadron level⁹² increase f_d of the soft pion contribution substantially (to around -1.6). This is close to the experimental value extracted from p-wave amplitudes. For the s-waves the f_d ratio is further enhanced to around -2.2 or even -2.5 by the SU(3) symmetry breaking in energy denominators of the intermediate states.⁹³

In fact, under certain assumptions a value of -1.6 for the f_d ratio of the soft pion contribution has been determined phenomenologically by Pham.⁹⁴ His determination raises further doubts as to the validity of the previous decompositions^{82,90} in which the value $(f_d)_{\text{soft pion}} = -1$ was used. The bigger value of the soft-pion f_d ratio was utilized in a recent update on the pole model by Nardulli.⁸³ His decomposition of the amplitudes again differs significantly from LeYaouanc et. al.⁹⁰ and Bonvin.⁸² In view of the uncertainties just discussed, a recent claim⁹⁵ that nonleptonic hyperon decays can be well understood should be considered as over optimistic.

In conclusion, no generally agreed upon explanation of the f_d problem in NLHD exists. This situation is *one* of the reasons for the proliferation of various results for WRHD – all obtained in the framework of the same general theoretical scheme.

7.1.2 Weak radiative hyperon decays

As discussed in Section 6 the tensor coupling contribution from the intermediate $(70, 1^-) \frac{1}{2}^-$ baryons leads to the standard form, Eq. 3.9 of the parity violating coupling of photon to baryons. Estimates of the contribution from the $\frac{1}{2}^-$ baryons were

performed by many workers⁹⁶⁻¹⁰⁰ at the time when the CERN experiment²⁵ was being carried out and again, more recently^{83,101,102} when a new wave of experimental results became imminent. Originally, the most extensive calculations were performed by Gavela et al.⁹⁶ To find out the contribution from the $\frac{1}{2}^-$ baryons, they evaluated the parity-conserving $\frac{1}{2}^- \rightarrow \frac{1}{2}^+ \gamma$ s-wave decay amplitudes in the quark model following the old Copley et al. method¹⁰³ and identified the results with the phenomenological couplings $f_{BB^*\gamma}$ in Eq. 6.8.

For the particular decay $\Sigma^+ \rightarrow p\gamma$, nonvanishing contributions come from $N^{*+}(\frac{1}{2}^+)$ (Fig. 6.1a) and $\Sigma^{*+}(\frac{1}{2}^+)$ (Fig 6.1b) members of the $(70, 1^-)\frac{1}{2}^-$ multiplet.

In the limit of exact SU(3) one has

$$\begin{aligned} f_{pN^{*+}\gamma} &= f_{\Sigma^+\Sigma^{*+}\gamma} \\ b_{N^{*+}\Sigma^+} &= b_{\Sigma^+p} \end{aligned} \quad (4)$$

Using Eq. 6.9 and Eq. 6.3, one obtains then that in the SU(3) limit these two contributions cancel each other in expression Eq. 6.11. In this way, contributions from tensor couplings $f_{BB^*\gamma}$ satisfy Hara's theorem. Since the parity conserving $\Sigma^+ \rightarrow p\gamma$ amplitudes in the pole model are proportional to the difference $\mu_{\Sigma^+} - \mu_p$ of baryon magnetic moments (i.e., $f_{BB^*\gamma}$ in Eq 6.15), the final result for the asymmetry and the branching fraction of the $\Sigma^+ \rightarrow p\gamma$ decay is very sensitive to the value of $\mu_{\Sigma^+} - \mu_p$, a feature already observed by Farrar.⁵³ Thanks to the fact that the experimental value for $\mu_{\Sigma^+} - \mu_p$ is significantly bigger than the quark model result, Gavela et al.⁹⁶ were able to obtain a large negative $\Sigma^+ \rightarrow p\gamma$ asymmetry. (This would not have been the case had they used the physical Σ^+, p masses and the additive quark model for the evaluation of μ_{Σ^+}, μ_p .) This and other results of Gavela et al.⁹⁶ are compared with the results of later experiments (see Table 2.1) in Table 7.1a (branching fractions) and Table 7.1b (asymmetry parameters). It is seen that their predictions went wrong in several places.

The contributions of the Σ^* and N^* resonances to the parity violating $\Sigma^+ \rightarrow p\gamma$ amplitude have also been estimated in the bag model.¹⁰⁰ As in Gavela et al.⁹⁶, Hara's theorem was satisfied by the cancellation of the contributions from these two resonances. Despite such similarities, the overall size of the parity violating and parity conserving amplitudes was found to be over an order of magnitude smaller than experimentally observed.

One may wonder if contributions from other intermediate states such as decuplet baryons could not bring theory in agreement with experiment. This does not seem to be the case, however. First, in the quark model such contributions vanish since the decuplet wave function is symmetric.^{79,90} Second, explicit considerations of decuplet contribution by Scadron and Thebaud¹⁰⁴ have yielded predictions that totally disagree with the present data on WRHD.

Table 7.1a Branching fractions (in units of 10^{-3}) of weak radiative decays: comparison of theoretical predictions with experiment.
Input entries are underlined.

	Gavela ⁹⁶	Gilman ⁷⁵	Kamal ¹⁰⁶		Verma ¹⁰⁷		Verma ¹	Zenc ¹⁰⁸	VDM Update	experiment
			A	B	(cq)	(ld)				
$\Sigma^+ \rightarrow p\gamma$	$0.92^{+0.26}_{-0.14}$	<u>1.24</u>	<u>1.24</u>	<u>1.24</u>	1.20	1.37	<u>1.24</u>	1.26	1.3-1.4	1.23 ± 0.06
$\Lambda \rightarrow n\gamma$	0.62	22.0	5.97	1.70	0.95	1.66	1.62	1.00	1.4-1.7	1.63 ± 0.14
$\Xi^0 \rightarrow \Lambda\gamma$	3.0	4.0	1.80	1.36	0.36	0.57	0.5	1.03	0.9-1.0	1.06 ± 0.16
$\Xi^0 \rightarrow \Sigma^0\gamma$	7.2	9.1	1.48	0.23	4.43	4.06	3.30	3.83	4.0-4.1	3.56 ± 0.43
$\Xi^- \rightarrow \Sigma^-\gamma$		11.0	1.20	1.20	<u>0.23</u>	<u>0.23</u>	<u>0.23</u>	0.29	0.15	0.128 ± 0.023
$\Omega^- \rightarrow \Xi^-\gamma$		41.	0.60	0.60	0.52	0.52	0.86		0.55 ± 0.20	< 0.46

Table 7.1b Asymmetries of weak radiative decays: comparison of theoretical predictions with experiment
Input entries are underlined.

	Gavela ⁹⁶	Kamal ¹⁰⁶		Verma ¹⁰⁷		Verma ¹	Zenc ¹⁰⁸	VDM Update	experiment
		A	B	(eq)	(ld)				
$\Sigma^+ \rightarrow p\gamma$	$\begin{smallmatrix} +0.32 \\ -0.80 \end{smallmatrix}$ -0.19	<u>-0.5</u>	<u>-0.5</u>	-0.59	-0.55	-0.56	-0.97	-0.95	-0.76 ± 0.08
$\Lambda \rightarrow n\gamma$	-0.49	-0.87	+0.25	-0.66	-0.52	-0.54	+0.76	+0.8	
$\Xi^0 \rightarrow \Lambda\gamma$	-0.78	-0.96	-0.45	+0.87	+0.74	+0.68	+0.65	+0.8	$+0.43 \pm 0.44$
$\Xi^0 \rightarrow \Sigma^0\gamma$	-0.96	-0.3	-0.99	-0.90*	-0.81*	-0.94	-0.36	-0.45	$+0.20 \pm 0.32$
$\Xi^- \rightarrow \Sigma^-\gamma$		-0.87	+0.56	<u>± 0.44</u>	<u>-0.44</u>	-0.60	+0.63	+0.7	$+1.0 \pm 1.3$
$\Omega^- \rightarrow \Xi^-\gamma$		-0.87	+0.56	+0.44	-0.44	-0.60		+0.7	

*Verma¹⁰⁷ erroneously reports a positive sign here, corrected later in Verma¹